Continental Shelf Research 60 (2013) 70–86

Contents lists available at SciVerse ScienceDirect

Continental Shelf Research

journal homepage: www.elsevier.com/locate/csr

Research papers

Surface distribution of brachyuran megalopae and ichthyoplankton in the Columbia River plume during transition from downwelling to upwelling conditions

G. Curtis Roegner [a,*], Elizabeth A. Daly [b], Richard D. Brodeur [c]

[a] Northwest Fisheries Science Center, National Marine Fisheries Service, National Oceanic and Atmospheric Administration, Point Adams Research Station, P.O. Box 155, Hammond, OR 97121, USA

[b] Cooperative Institute for Marine Resources Studies, Oregon State University, Hatfield Marine Science Center, 2030 S. Marine Science Drive, Newport, OR 97365, USA

[c] Northwest Fisheries Science Center, National Marine Fisheries Service, National Oceanic and Atmospheric Administration, 2030 SS. Marine Science Drive, Newport, OR 97365, USA

ARTICLE INFO

Article history:
Received 10 July 2012
Received in revised form
19 March 2013
Accepted 3 April 2013
Available online 19 April 2013

Keywords:
Columbia River plume
Crab megalopae
Juvenile fishes
Neuston
Upwelling
California Current

ABSTRACT

In the California Current coastal boundary zone, the spring transition between downwelling and upwelling conditions, along with the fluctuating structure of the Columbia River plume, creates highly dynamic interactions. In this study, we investigated whether the surface distribution of brachyuran larvae and ichthyoplankton would track the dynamics of the Columbia River plume. By happenstance, the cruise period coincided with the spring transition from downwelling to sustained upwelling conditions in 2010, a year when the transition was delayed and Columbia River flow was substantially higher than average. We used time series of wind and freshwater input to evaluate the influence of physical forcing on oceanographic patterns, and sampled hydrography and surface plankton concentrations within a 182 km^2 grid off Willapa Bay, WA. Additionally, two longer transects, one cross-shelf and the other along-shore, were made to discern the extent of plume influence on larval crab and fish abundance. We found that plume waters that were trapped in a northward-flowing coastal-boundary current during downwelling conditions were advected offshore after several days of upwelling-favorable winds. Neustonic collections of brachyuran larvae and ichthyoplankton varied in response to this large seaward advective event. Megalopae of cancrid crabs exhibited patterns of both offshore transport (*Cancer oregonensis/productus*) and nearshore retention (*C. magister*). Additionally, abundant numbers of large juvenile widow (*Sebastes entomelas*) and yellowtail (*S. flavidus*) rockfish of a size appropriate for settlement were sampled during a period when ocean conditions favored high recruitment success. These results demonstrated that the response of planktonic crab larvae and ichthyoplankton to large-scale advection varied by species, with larger and more vagile fish exhibiting less evidence of passive transport than smaller crab larvae. Importantly, portions of the planktonic fish and crab community were able to maintain nearshore distributions in favorable settlement habitat, despite physical advection offshore.

Published by Elsevier Ltd.

1. Introduction

The Columbia River exerts a large influence on the oceanography of the Northeast Pacific Ocean. It is by far the largest source of freshwater to the Northern California Current (NCC), and its plume interfaces with a major upwelling center (the California Current Large Marine Ecosystem) producing strong biophysical gradients. Wind stress, river flow, and tidal forcings all contribute to the dynamics of plume orientation, surface stratification, and vertical and horizontal mixing (Hickey et al., 1998; Hickey and Banas, 2003). These physical factors in turn influence biotic features such as phytoplankton blooms (Roegner et al., 2002), zooplankton species composition and concentration (Roegner et al., 2003; Morgan et al., 2005; Peterson and Peterson, 2008), and the distribution and migratory pathway of anadromous and marine fish (De Robertis et al., 2005; Emmett et al., 2006). Recent investigation of physical features of the Columbia River plume has led to greater understanding of plume dynamics (Hickey et al., 2010). However, the responses of biota to rapidly changing physical conditions typical of those in the Columbia River plume have rarely been assessed.

The Columbia River plume is composed of a series of ebb-flow injections of freshwater to the coastal ocean, which are mixed with ocean water by wind and tidal forces. The *near-field* plume

* Corresponding author. Tel.: +1 503 861 1818.
E-mail address: Curtis.Roegner@noaa.gov (G.C. Roegner).

0278-4343/$ - see front matter Published by Elsevier Ltd.
http://dx.doi.org/10.1016/j.csr.2013.04.007

has been defined as recently outwelled water, and the *far-field* plume as older waters that have been altered to various degrees by mixing (Horner-Devine et al., 2009). Wind stress plays a fundamental role in plume structure and direction, and in spring and summer, oscillating north–south winds generate predicable variation in the state of the plume (Hickey et al., 2005). Downwelling (poleward) winds concentrate and thicken buoyant plume water along the Washington coast, where it is driven north as far as the Juan de Fuca Strait and eddy (Hickey et al., 2009) and is regularly advected into coastal estuaries (Roegner et al., 2002; Banas et al., 2007). With a change to upwelling-favorable (equatorward) winds, new plumes are driven offshore and to the southwest by Ekman transport, where they spread and thin. Sufficient upwelling wind stress will also cause the northward-tending plume along the Washington coast to be replaced by upwelled subsurface water (Roegner et al., 2002; Hickey et al., 2005). The transition between downwelling and upwelling winds, and the resulting change in orientation of both near- and far-field plumes, can occur over the course of a few days, and result in dramatic change in biological and physical oceanographic conditions (Roegner et al., 2002, 2003; Hickey et al., 2009).

There has long been interest in the recruitment dynamics of nearshore and shelf-residing brachyuran crabs and fishes in the California Current, and particular attention has focused on mechanisms to explain recruitment variation during coastal upwelling-relaxation cycles (Roughgarden et al., 1988; Shenker, 1988; Shanks, 1995; Shanks and Eckert, 2005). Wind-forced upwelling tends to move surface waters offshore, and potentially away from optimal shallow-water settlement sites. Recent studies of intertidal and nearshore invertebrates have shown that behavioral adaptions can aid avoidance of offshore advection and serve to retain larvae near the coast (Shanks and Shearman, 2009; Morgan et al., 2009a, b). However, the larvae or pelagic juveniles of many species inhabit the neuston layer (defined as the upper 1 m of the ocean), either as obligate residents that remain at the surface until larval settlement, or more commonly as facultative residents that employ diurnal, tidal, or ontogenetic vertical migration to move between surface and sub-surface layers (Shenker, 1988; Hobbs and Botsford, 1992; Queiroga and Blanton, 2005). Vertical position in vertically sheared flow has major ramifications for larval dispersion and recruitment (Hill, 1995; Roughan et al., 2005; Morgan et al., 2009a). The surface layer in particular is often subjected to wind-forced advection that can transport larvae in trajectories that diverge substantially from those of subsurface layers (Hobbs and Botsford, 1992).

Invertebrate and fish larvae in the CCS appear to have evolved a diversity of reproductive and dispersal strategies that facilitate coastal and nearshore recruitment, especially in coordination with major seasonal oceanographic regimes (Shanks, 1995; Shanks and Eckert, 2007; Shanks and Roegner, 2007). However, few organisms in the PNW have evolved to develop their entire life cycles within the rapidly changing physical conditions of the Columbia River plume; rather they are entrained in plume water through passive mixing or by active vertical migration. Limited observations exist on short-term variation of plankton distribution in relation to physical forcing in the Columbia River plume, and there are few data to determine the effect of plume advection on dispersal from suitable settlement habitats (Doyle, 1992a).

Are larvae advected offshore with plume water during upwelling events? We hypothesized that the surface distribution of brachyuran larvae and ichthyoplankton would track the dynamics of the Columbia River plume. In this study we present data from a small-scale, intensely sampled grid of stations, as well as data from longer cross-shelf and along-shore transects, that were collected during a reversal in wind direction with subsequent changes in water mass structure. These event-scale observations aid in understanding the fate of meroplanktonic organisms under strong advective forcing.

2. Methods

2.1. Time series measurements from moorings

We used time series of wind and freshwater input to evaluate the influence of physical forcing on oceanographic patterns and larval abundance. Mean daily alongshore wind stress (N m^{-2}) was determined from wind vectors recorded at Columbia River buoy 46029 (124.5°N, 46.1°W; Fig. 1). Poleward (southerly) winds lead to downwelling, and equatorward (northerly) winds generate upwelling circulation patterns in the California Current System. We calculated the 4-d cumulative wind stress as an index to assess trends in wind forcing. Freshwater input to the ocean near the sample site was estimated from Columbia River and Willapa Bay watersheds. For the Columbia River flow, we plotted mean daily flow volume and the 10-yr average mean daily flow volume (Q, m^3 s^{-1}) at Bonneville Dam (CRDART, 1995). For the Willapa system (which is directly inshore of the sampling region), we examined time series of mean daily stream flow from the U.S. Geological Survey Naselle and Willapa River gauging stations (USGS, 2006).

We also estimated stage of tide during ocean sampling from water levels recorded at NOAA tidal station 9439040 (Astoria, 46.21°N, 123.21°W). Stage of tide was calculated by assigning 1 to high water and 0 to low water, and partitioning time intervals between highs and lows. Periods of flooding water were assigned positive values, and periods of ebbing water were defined with negative values (e.g. 0.5 corresponds to mid-flood tide, while −0.5 is mid-ebb tide). We employed a lag of −1.5 h to account for delay in the propagation of tidal waves from the ocean to the estuary.

2.2. Cruise transects

We sampled hydrography and plankton from the NOAA R/V *Miller Freeman* during 9–15 June 2010. The primary cruise plan entailed repeated cross-shelf transects within a 182 km^2 grid of 16

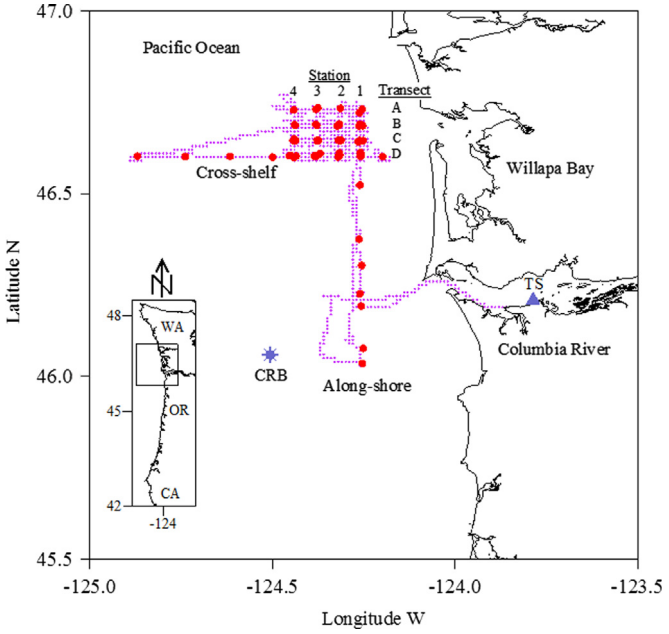

Fig. 1. Cruise track of R/V *Miller Freeman* during 9–15 June 2010, showing the sampling grid, cross-shelf and along-shore transects. CRB=Columbia River NOAA weather buoy 46029. TS=Tongue Point tide station. Inset shows regional setting.

stations off Willapa Bay, Washington (bounded by 47.73–46.60°N and 124.25–124.44°W; Fig. 1), in order to access nightly variation in plankton composition. Stations within the grid were separated by 4.6 km, and the innermost stations were 12.1–14.3 km from shore; depths within the grid ranged from 43 to 103 m. Each night during 9–13 June 2010, we surveyed as many stations as possible within the grid between the hours of ~2100 and 0600 h. A total of thirteen 13.9-km transects were sampled over four nights (Grids I-IV).

Secondarily, we made two longer transects to discern the extent of plume influence on larval crab and fish abundance (Fig. 1). The first was a cross-shelf transect initiated on 14 June that began along transect *D* (46.6°N) and extended 60.9 km offshore to 124.87°W. Station intervals varied from 4.6 to 9.7 km and depths from 38 to 913 m. The second was a 77.7-km along-shore transect that extended from north of the mouth of Willapa Bay (46.72°N, 124.26°W) to south of the mouth of the Columbia River (46.03°N, 124.25°W). Station interval here varied from 4.7 to 16.4 km, and depths ranged from 51 to 101 m and were conducted at night.

2.3. Oceanographic measurements

A continuous underway time series of near-surface (5-m) salinity and temperature was provided by a flow-through thermo-salinograph that recorded at 1 min intervals (Seabird Electronics SBE 21).[1] Salinity data were contoured into surface plots (1.0 anistropy) for each of the four grids. We also plotted salinity by longitude (grids and cross-shelf transect) or latitude (along-shore transect) to provide spatial determination of the plume and upwelling conditions. Salinity and temperature values at the time of net tows were extracted from the data set (statistical analyses described below). We also used the 5-m salinity data to determine the location of frontal regions relative to neuston net tows (described below). Frontal zones were identified by first computing the mean salinity in 5-min intervals and then calculating the change in mean salinity per interval ($\delta S/t$). From these data we generated scatter plots of the salinity gradient with larval concentration.

Water column structure during along- and cross-shelf transects was measured with a Seabird Model 25 conductivity–temperature–depth (CTD) profiler equipped with Wet Labs fluorometer and oxygen sensors. The CTD profiler sampled from near-surface to a depth within 5 m of the bottom on the shelf and to a maximum depth of 100 m elsewhere. For the purposes of this study, we concentrated primarily on salinity in the upper 25-m of the water column. Profiles were averaged into 1-m intervals (38.7 ± 18.2 sd measurements per bin), and transect profiles were contoured into distance-depth plots employing circular kriging with anisotropy = 0.01 (Golden Software, Surfer v10).

Because light is a major cue for vertical migration behavior, we measured ambient light intensity (lux) at 30-min intervals (Onset Instrument Corp. UA-002-64). Sunset/sunrise occurred at ~2000/0430 h bracketed by 39 min of civil twilight. For reference, light intensity at sunrise on a clear day is about 400 lx. Sampling occurred during a new moon period with lunar illumination between 0 and 20%.

2.4. Neuston net tows

Surface distributions of fish and crab were sampled with a Manta-style neuston net identical to that used by Roegner et al. (2003) and Morgan et al. (2005) (1.5×0.5-m^2 mouth; 300-μm mesh). The neuston net was towed for 5 min at ~1 m s^{-1}, and the volume of water filtered was determined with a General Oceanics flowmeter (average 231.1 ± 30.2 m^3). All brachyuran megalopae and all fish larvae and juveniles in the samples were identified to lowest taxon possible. Some taxa, such as smaller members of the brachyuran crab genus *Cancer* and rockfishes of the genus *Sebastes*, were difficult to identify using only morphometric or meristic characteristics; therefore, we left these at the generic level for this analysis. Catch was standardized by filtered volume to yield concentration, *C* (individuals m^{-3} for brachyurans; individuals 10^3 m^{-3} for the less abundant fish).

2.5. Statistical methods

For both crab and fish data, we used the following descriptive statistics to evaluate larval distributions by sample period: mean concentration (C = individuals per m^3 for crab and individuals per 10^3 m^3 for fish), concentration skewness (γ, where 0 skewness indicates a normal distribution), and larval frequency of occurrence (FO, the proportion of non-zero tows). We used analysis of variance (ANOVA) and the Tukey post-hoc procedure to test for differences in mean larval concentration among sampling periods. We generated a correlation matrix to examine linear relationships between neuton concentrations and the environmental variables light intensity, hours relative to sunset, temperature, salinity, and stage of tide.

To estimate total numbers of crab larvae among grids, we contoured larval concentration data into surface plots (1.0 anisotropy), integrated the plots by area, and standardized abundance to a 100 km^2 area. Ichthyoplankton were too sparse for this analysis.

Non-parametric multiplicative regression (NPMR) analysis was used to examine relationships between dominant taxa sampled in the neuston and the environmental variables of hours from sunset, stage of tide, temperature, and salinity. Light levels based on lux covaried with hours from sunset; therefore, we ran initial models with both variables. Model fit improved for data with increased hours from sunset, so we used these data for NPMR analysis. Best-fit models were created using a local linear estimator with a predictor ratio minimum of 5; no improvement criteria; a minimum average neighborhood size of n (samples) $\times$ 0.03; and a step size of 5% of the range. We also used a 10% maximum allowable limit for missing estimates; a minimal backtracking search method; and a leave-one-out cross-validation. Statistical significance for each model was evaluated after 1000 runs. All NPMR analyses were performed using the statistical software HyperNiche Version 2.2 (McCune and Mefford, 2009).

A non-metric multidimensional scaling (MDS) ordination was used to examine patterns of community structure in the neuston for each station along the four sampling grids (I-IV). We excluded zero-catch stations ($n = 3$) and, based on initial MDS plots, outlier stations where only one crab or fish was caught ($n = 5$). Abundance data was $\log(x+1)$ transformed prior to analysis to achieve normality. Separation of the ordination was determined by stress value, where values > 2.0 indicated low structure and those < 1.5 suggested good separation (Clarke, 1993). To test for significant differences in the fish and crab community between grids ($p < 0.05$), we used one-way analysis of similarity (ANOSIM), a non-parametric multivariate analog to analysis of variance, which is based on the matrix of pairwise Bray–Curtis similarity coefficients (Clarke, 1993). The resulting global R statistic ranges from 0 to 1, where 0 indicates no separation and 1 indicates complete separation among groups. All multivariate analyses were done using PRIMER-E v6 (Clarke and Gorley, 2006).

[1] Reference to trade names does not imply endorsement by the National Marine Fisheries Service, NOAA.

3. Results

3.1. Time series measurements

Columbia River stage was below average in the months preceding the cruise but increased rapidly during the cruise and reached peak flow of the annual freshet with a maximum flow volume (Q) of ~11000 $m^3 s^{-1}$ (Fig. 2a). This rate was 1000–4000 $m^3 s^{-1}$ larger than the 10-year average for that time of year. Combined Q from the two largest rivers entering Willapa Bay was minimal in comparison (~30 $m^3 s^{-1}$), and likely had a negligible effect on salinity patterns at the study site.

Winds were downwelling-dominant for 17 d preceding the cruise, and turned weakly upwelling-favorable 5 d before the cruise (Fig. 2b). Equatorward wind stress then increased in intensity and peaked at −0.21 N m^{-2} on 14 June, midway through the cruise (Fig. 2c). Thereafter, winds reduced in intensity but maintained an upwelling-favorable direction. The 4-d cumulative wind stress reached a maximum upwelling-favorable intensity during day 5 of the cruise.

Tides at Astoria were unequal spring tides, with the larger ebb occurring during nighttime hours (Fig. 2d). Six large and six small tidal plumes were generated during the study period. Nighttime sample collection varied relative to the tidal cycle. Grid I samples were collected mostly during the large ebb tide, while the final alongshore transect began around slack low water, continued through the flood tide, and finished during mid-ebb tide, when sampling was near the mouth of the Columbia.

3.2. Vertical plume structure

Plume water (defined as salinity < 31) was detected at the sea surface during all sample periods, while ocean water (salinity ≥31) was rarely measured above 5 m. The plume was highly stratified with vertical salinity gradients in the upper 20 m of up to −0.77 m^{-1}. Maximum depth of the plume was 19 m, while water of salinity < 25 was confined to the surface 5 m. All CTD samples collected at depths between the surface and 25 m had normoxic oxygen values (> 8 mg L^{-1}) and low chlorophyll fluorescence (< 2 μg L^{-1}). However, the distribution of low-salinity water was dynamic during the study period, as described below.

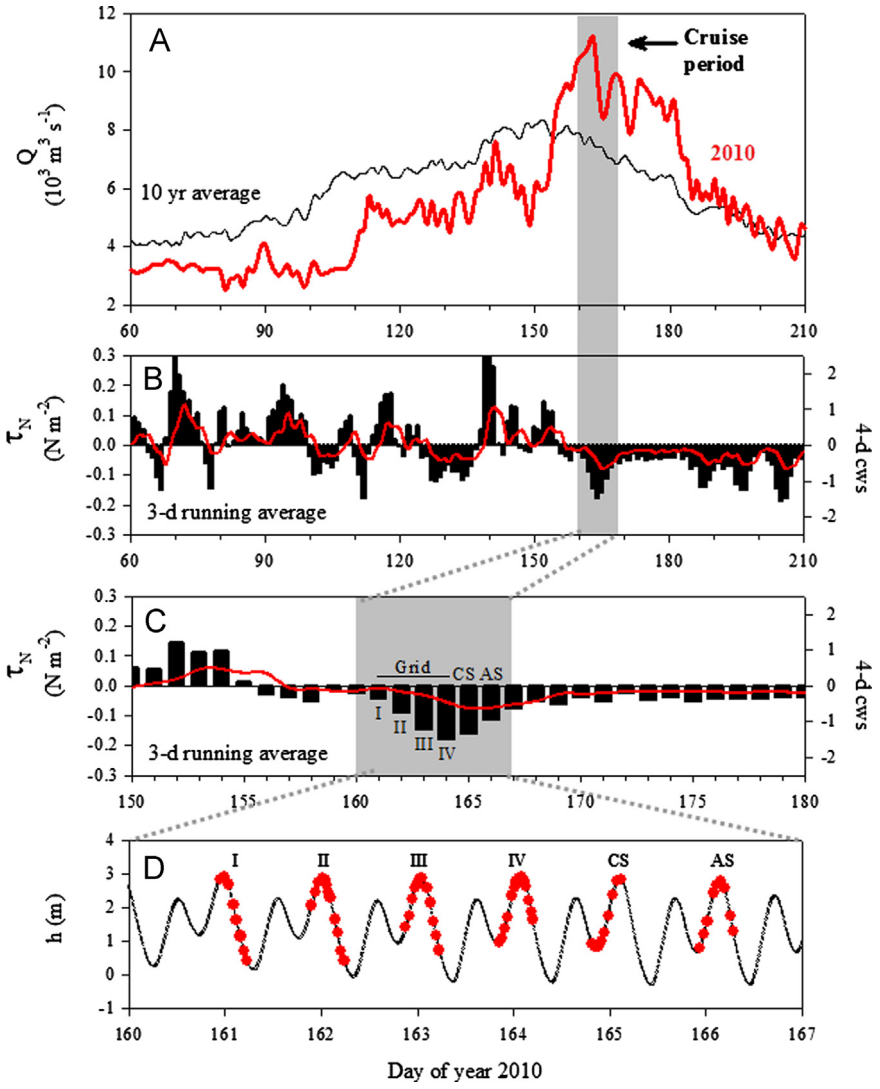

Fig. 2. Time series of physical variables for periods surrounding the cruise dates (gray shading). (A) Columbia River stream flow during 1 March-29 July 2010 (thick) compared to the 10-year average (thin). (B). Time series of low-pass filtered mean daily (bars) and 4-d cumulative mean daily (line) wind stresses during 1 March-29 July 2010. (C) Plot B detail for the period 30 May–29 June. Letters denote grid (I–IV), cross-shelf (CS), and along-shore (AS) transects. (D) Semidiurnal tidal fluctuations (black line) in relation to neuston tow samples (symbols) during the cruise period. Transects delineated as in C.

3.3. Overall abundance of crab megalopae and larval and juvenile fish

We made 64 neuston tows. Megalopae of three brachyuran crab species were present in surface water samples during the cruise period (Table 1). Overall, the Dungeness crab, *Cancer magister*, was both abundant and widespread ($n=3521$; mean $C \pm \text{sd} = 0.24 \pm 0.25$ individuals m^{-3}; $\gamma=1.37$; FO=0.92). *Cancer oregonensis/productus* (taxonomic segregation difficult) was less abundant and more patchy ($n=804$; $C=0.06 \pm 0.11$; $\gamma=3.23$; FO=0.71). Purple shore crab (*Hemigrapsus nudus*) megalopae were found in low concentration and at fewer stations ($n=75$; $C<0.01 \pm 0.02$; $\gamma=4.20$; FO=0.25). We counted 75 unidentified crab zoea and three megalopae of the anomuran mole crab *Emertia analoga*.

Abundance of fish was typically 10–100 times lower than abundance of *C. magister* megalopae, and we standardized concentrations to a volume of 10^3 m^3 (Tables 1 and 2). Overall, fish larvae and juveniles were moderately abundant and well-distributed, but concentration was patchy ($n=207$; mean $C=13.6 \pm 12.6$; $\gamma=4.0$; FO=0.81; Table 2). The most frequently caught and widespread fish were juvenile rockfishes *Sebastes* spp., the majority of which were yellowtail (*S. flavidus*) or widow rockfish (*S. entomelas*; $n=62$; $C=4.2 \pm 6.4$; $\gamma=8.0$; FO=0.46), followed by juvenile ronquils *Ronquilis jordani* ($n=56$; $C=3.6 \pm 6.0$; $\gamma=7.0$; FO=0.37). Other fishes found in the neuston were juvenile kelp greenlings (*Hexagrammos decagrammus*), larval and juvenile sculpins (Cottidae), larval smelt (Osmeridae), and juvenile Pacific sandlance (*Ammodytes hexapterus*), along with several other infrequently encountered taxa (Fig. 5). Aside from megalopae and fish, few other organisms that exceeded 1 mm were present in the samples (including gelatinous zooplankton).

Average fork length of neustonic fish was 40.4 ± 15.5 mm, which most likely reflected the transformed juvenile stages. One 12-mm larval rockfish was sampled, and the remaining rockfish were large pelagic juveniles ranging from 43 to 62 mm for an overall mean fork length of 53.6 ± 6.7 mm (Table 2). For juvenile ronquil and osmerid, average fork lengths were 27.3 ± 5.0 mm and 36.8 ± 2.5, respectively. Also sampled in the neuston were large juvenile Pacific sandlance (56.2 ± 9.0 mm) and kelp greenlings (57.0 ± 8.4 mm). All the smallest fish sampled (<15 mm) were caught during the last two days of sampling and were mainly larval sculpins.

3.4. Grid sampling—oceanography and biota

We sampled two complete transects (eight stations) during the night of 9–10 June (Fig. 3, Grid I). Mean ($\pm$ sd) surface salinity in the sample grid was 27.7 ± 1.6, indicating we were sampling plume water. However, horizontal salinity distribution was uneven, with the most southern transect (transect *D*) exhibiting the strongest surface-salinity gradient that increased offshore, while transect *C* salinities were higher and more constant. The 5-m surface-salinity plot showed a lobe of low-salinity plume water along the southern transect.

C. magister megalopae were found at all stations in high concentrations with a relatively even distribution except in the sample made during twilight ($C=0.03$ at 64.6 lx; Fig. 4; Table 1). *C. oregonensis/productus* megalopae also had high frequency of occurrence (FO=1.0), and a high and relatively even concentration with wide distribution. The highest concentrations of *C. oregonensis/productus* megalopae were present in higher salinity water at the outer two stations of both transect lines.

Fish concentrations in Grid I were the lowest among all grids, few or no fish were present at lower-salinity stations, and no fish were collected from the station sampled at twilight (Fig. 4; Table 2).

Table 1
Catch statistics for brachyuran larvae captured in neuston tows.

Species	Survey and number of tows (*N*)	Ind. (*n*)	Concentration (individuals m^{-3})			Skewness (γ)	FO
			Mean (sd)	Min	Max		
Grids I–IV							
Cancer magister	Grid I (8)	781	0.47 (0.31)	0.03	0.91	0.24	1.00
	Grid II (12)	1196	0.46 (0.29)	0.02	1.06	0.48	1.00
	Grid III (13)	344	0.11 (0.10)	0	0.28	0.32	0.77
	Grid IV (13)	387	0.12 (0.11)	0	0.40	1.50	0.86
Cancer spp.	Grid I (8)	411	0.25 (0.22)	0.04	0.56	0.44	1.00
	Grid II (12)	103	0.04 (0.05)	0	0.15	1.29	0.92
	Grid III (13)	24	0.01 (0.01)	0	0.03	1.46	0.62
	Grid IV (13)	110	0.03 (0.04)	0	0.12	0.99	0.79
Hemigrapsus nudus	Grid I (8)	11	0.01 (0.01)	0	0.02	1.18	0.38
	Grid II (12)	26	0.01 (0.02)	0	0.07	2.34	0.17
	Grid III (13)	1	0.01 (0.00)	0	<0.01	3.61	0.08
	Grid IV (13)	6	0.01 (0.00)	0	0.01	1.57	0.21
Cross-shelf and alongshore transects							
Cancer magister	CS (9)	339	0.16 (0.21)	0	0.71	2.48	0.89
	AS (9)	474	0.21 (0.18)	0	0.45	0.02	0.78
Cancer spp.	CS (9)	132	0.07 (0.06)	0	0.15	0.15	0.78
	AS (9)	24	0.01 (0.03)	0	0.09	2.84	0.67
Hemigrapsus nudus	CS (9)	1	<0.01 (0.00)	0	0.08	3.00	0.11
	AS (9)	30	0.01 (0.03)	0	<0.01	2.50	0.33
Total or overall average							
Cancer magister		3521	0.24 (0.25)	0	1.06	1.37	0.92
Cancer spp.		804	0.06 (0.11)	0	0.56	3.23	0.71
Hemigrapsus nudus		75	<0.01 (0.02)	0	0.09	4.20	0.25

Values shown are for grid stations (I–IV), cross-shelf and alongshore extended transects, and totals for the sampling period. Abbreviations: Ind., individuals; FO, frequency of occurrence; CS, cross-shelf and AS, alongshore. *Cancer* spp*: Cancer oregonensis/productus.*

Table 2
Catch statistics for ichthyoplankton captured in neuston tows.

Species	Survey area and number of tows (n)	Ind. (n)	Concentration (individuals 10^3 m^{-3})			Skewness (γ)	FO	Standard length (mm) and sd
			Mean (sd)	Min	Max			
Grids I–IV								
All fish	Grid I (8)	9	5.50 (5.44)	0	13.72	0.4	0.63	43.8 (14.0)
	Grid II (12)	54	20.15 (12.30)	0	43.74	0.1	0.92	46.2 (14.8)
	Grid III (13)	36	11.5 (8.31)	0	23.15	0.1	0.85	34.8 (13.1)
	Grid IV (13)	32	9.77 (7.35)	0	23.83	0.5	0.86	37.4 (14.3)
Sebastes spp.	Grid I (8)	6	3.74 (4.47)	0	10.94	0.8	0.50	52.7 (4.3)
	Grid II (12)	25	8.96 (11.07)	0	35.79	2.0	0.58	54.9 (3.6)
	Grid III (13)	7	2.32 (4.34)	0	13.58	2.9	0.31	55.3 (4.8)
	Grid IV (13)	10	3.19 (4.43)	0	12.78	1.8	0.43	50.9 (5.0)
Ronquilis jordani	Grid I (8)	0	0	0	0	–	0.00	–
	Grid II (12)	12	4.60 (5.65)	0	18.72	2.2	0.58	25.4 (4.1)
	Grid III (13)	21	6.65 (7.71)	0	21.59	1.2	0.54	26.7 (5.1)
	Grid IV (13)	9	2.86 (3.71)	0	9.53	1.2	0.43	28.3 (4.7)
Cross-shelf and alongshore transects								
All fish	CS (9)	52	24.47 (18.64)	0	56.76	0.48	0.89	43.3 (15.7)
	AS(9)	24	10.43 (14.07)	0	43.32	2.3	0.67	32.5 (16.8)
Sebastes spp.	CS (9)	11	5.19 (5.45)	0	13.24	0.38	0.22	52.1 (13.4)
	AS(9)	3	1.24 (1.86)	0	3.94	1.1	0.44	55.3 (1.2)
Ronquilis jordani	CS (9)	4	1.78 (3.96)	0	11.61	2.9	0.56	24.0 (2.2)
	AS(9)	10	4.27 (8.97)	0	27.56	3.4	0.33	31.0 (4.9)
Total or overall average								
All fish		207	13.64 (12.64)	0	56.76	4.0	0.82	40.4 (15.5)
Sebastes spp.		62	4.15 (6.44)	0	35.79	8.0	0.4	53.6 (6.7)
Ronquilis jordani		56	3.63 (5.97)	0	27.56	7.0	0.6	27.3 (5.0)

Values shown are for grid stations (I–IV), cross-shelf and alongshore extended transects, and total or average for all surveys. Abbreviations: Ind., individuals; FO, frequency of occurrence; CS, cross-shelf and AS, alongshore.

The majority of fish sampled in Grid I were juvenile rockfishes and juvenile sculpins present at moderate to low concentrations (Fig. 5).

We completed three transects (12 stations) during the night of 10–11 June (Fig. 3, Grid II). Mean surface salinity decreased from the previous night to 25.0 ± 1.6, and the surface plot indicated low-salinity water in most of the sample grid with horizontal salinity gradients again increasing offshore (Fig. 4). As on the previous night, *C. magister* megalopae were found at every station. Concentrations remained high and evenly distributed, except the final two stations sampled during twilight when concentration decreased to <0.05 individuals m^{-3} (Fig. 4; Table 1). In contrast, *C. oregonensis/productus* megalopae decreased in abundance and distribution, and concentrations became more skewed.

Concentrations of total fish were found to be one of the highest of the study (Fig. 4; Table 2). Juvenile rockfishes (Table 2) and juvenile kelp greenlings were collected at their highest frequency of occurrence and abundance (Fig. 5). Ronquils were collected in their second highest abundance, and the catch of total fish at twilight was also high (Table 2).

Thirteen stations were sampled on 11–12 June (Fig. 3, Grid III). Surface salinity values remained low (25.8 ± 0.9) but tended to increase toward shore, suggesting offshore movement of the plume. The mean concentration of C. *magister* megalopae decreased markedly while maintaining a relatively even distribution Table 1) and FO decreased to 0.77. Concentrations of *C. oregonensis/productus* megalopae decreased below 0.01 individuals m^{-3} over the entire grid (only 24 individuals were sampled) and FO fell to 0.62. Total fish concentrations were moderate and juvenile ronquils were present at their highest abundance and frequency (Fig. 4; Table 2), while abundances of juvenile rockfish, osmerids, and kelp greenlings were reduced (Fig. 5).

The final grid sampling cruise included 14 stations (Fig. 3, Grid IV). Mean surface salinity increased to 28.0 ± 0.6. Gradients remained higher inshore, suggesting continued offshore advection of the far-field plume. C. *magister* megalopae concentrations remained lower with increased skewness and a slightly increased distribution (Fig. 4; Table 1). Concentrations tended to be high in higher-salinity, inshore water. Low concentrations of *C. oregonensis/productus* megalopae were found across the sampling grid. In contrast to the larval distribution of *C. magister*, fish were caught in fewer numbers in the higher-salinity inshore waters (Fig. 4; Table 2). Concentrations of larval osmerids and sculpins increased, while low to moderate concentrations of juvenile rockfishes and ronquils were collected (Fig. 5).

3.5. Offshore transect

On the night of 13–14 June, we continued offshore from transect *D* to sample an additional four stations. Salinity at the 5-m depth decreased with distance offshore, ranging from 30.7 inshore to 28.2 offshore (Fig. 6A). Isohalines from CTD casts sloped upward in plume water; however the 31 isohaline remained around 10 m, indicating deep upwelling had not been initiated.

C. magister megalopae were widely distributed across the shelf at moderately high concentrations and tended to increase with distance offshore, reaching a maximum concentration ($C=0.71$) at the most offshore station (60.9 km at the 645-m depth; Fig. 6A,

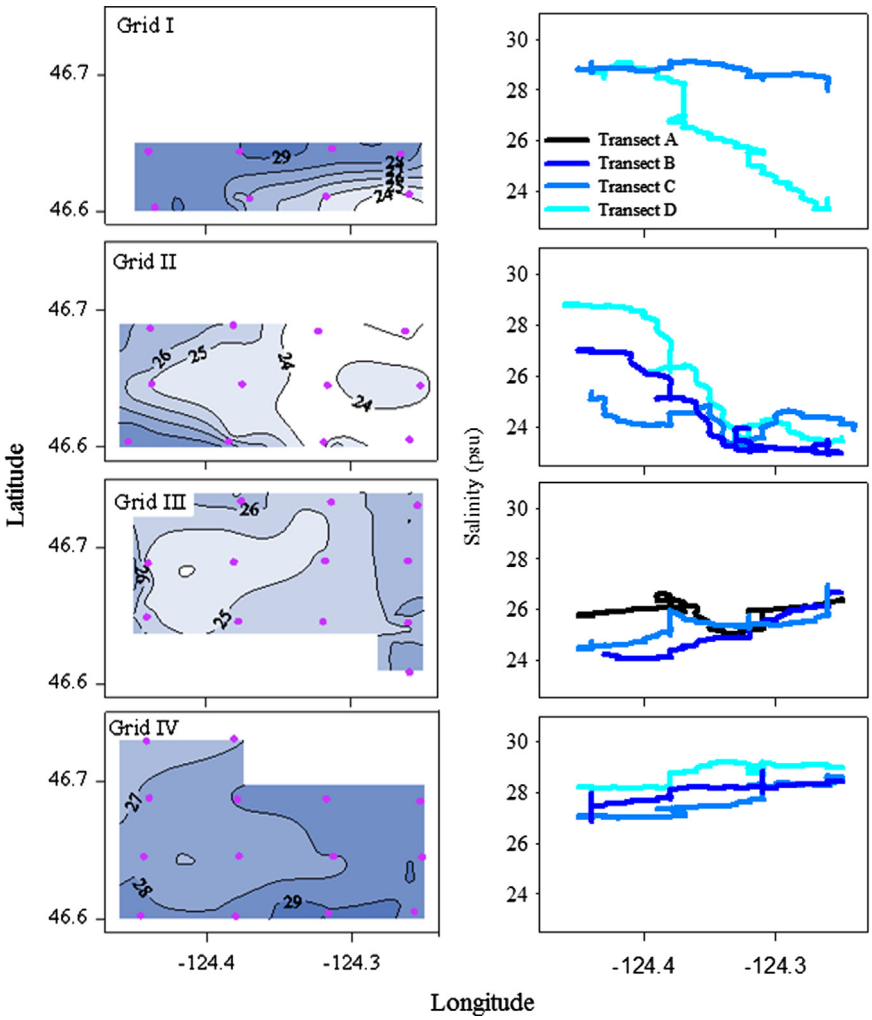

Fig. 3. Five-meter salinity measured during grid samples. (A) Interpolated surface distribution from CTD casts (isohalines = 1.0). (B) Continuous salinity during grid transects, illustrating the changing east-west salinity gradient.

Table 1). *C. oregonensis/productus* megalopae were also common along this transect at a low but evenly distributed concentration.

Fish concentrations were highest along the offshore transect than in any other area (Fig. 6A; Table 2), with high osmerid abundance at the inshore stations. Kelp greenlings, ronquils, rockfishes, sculpins, and sandlance were all caught in moderate concentrations at stations west of the grid (Fig. 5). The highest mean concentration of total fish was sampled at the western-most station primarily due to a high concentration of juvenile lanternfishes (Myctophidae; Fig. 5).

3.6. Alongshore transect

Finally, on the night of 14–15 June, we sampled along 124.26°W from north of Willapa Bay to south of the Columbia River mouth. Salinity at the 5-m depth north of the Columbia averaged 30.6 ± 0.4, indicating that most plume water had been replaced by higher-salinity water (Fig.6B). As we crossed the mouth of the Columbia and the near-field plume front, salinity dropped precipitously and fluctuated between 19 and 28. Isohalines from CTD casts show upwelling north of the estuary mouth, while the new plume was oriented south of the mouth (ship traffic precluded CTD or net tow samples in the main channel). These data indicate the far-field plume had moved offshore and the near-field plume had transited to a southwesterly orientation

C. magister megalopae were very evenly concentrated at moderate abundance along the transect, and were only absent in the last two samples made during twilight (Fig. 6B; Table 1). *C. oregonensis/productus* megalopae were not abundant along the cross-shore transect; overall concentration was low and patchy, and larvae were sampled primarily at the higher-salinity stations. Catches of fish were high only in the most northern stations of the transect, and few to zero fish were caught south of the sampling grid (Fig. 6B, Table 2). However, the highest concentration of larval sculpins of the study effort were caught during the alongshore transect, and moderate concentrations of ronquils and Pacific sandlance were also sampled (Fig. 5).

3.7. Plankton variations among grids

C. magister had significantly higher mean concentrations during sampling of Grids I and II than Grids III and IV or the cross-shelf transect (Fig. 7). Concentrations during the alongshore transect were intermediate and not significantly different from those seen during the previous nights. *C. oregonensis/productus* had a significantly higher concentration in samples from Grid I than in samples from other nights. Estimates of the total number of megalopae per 100 km^2 indicated a fivefold decrease in abundance of *C. magister* megalopae between the first two (Grids I and II) and second two (Grids III and IV) gird surveys, while

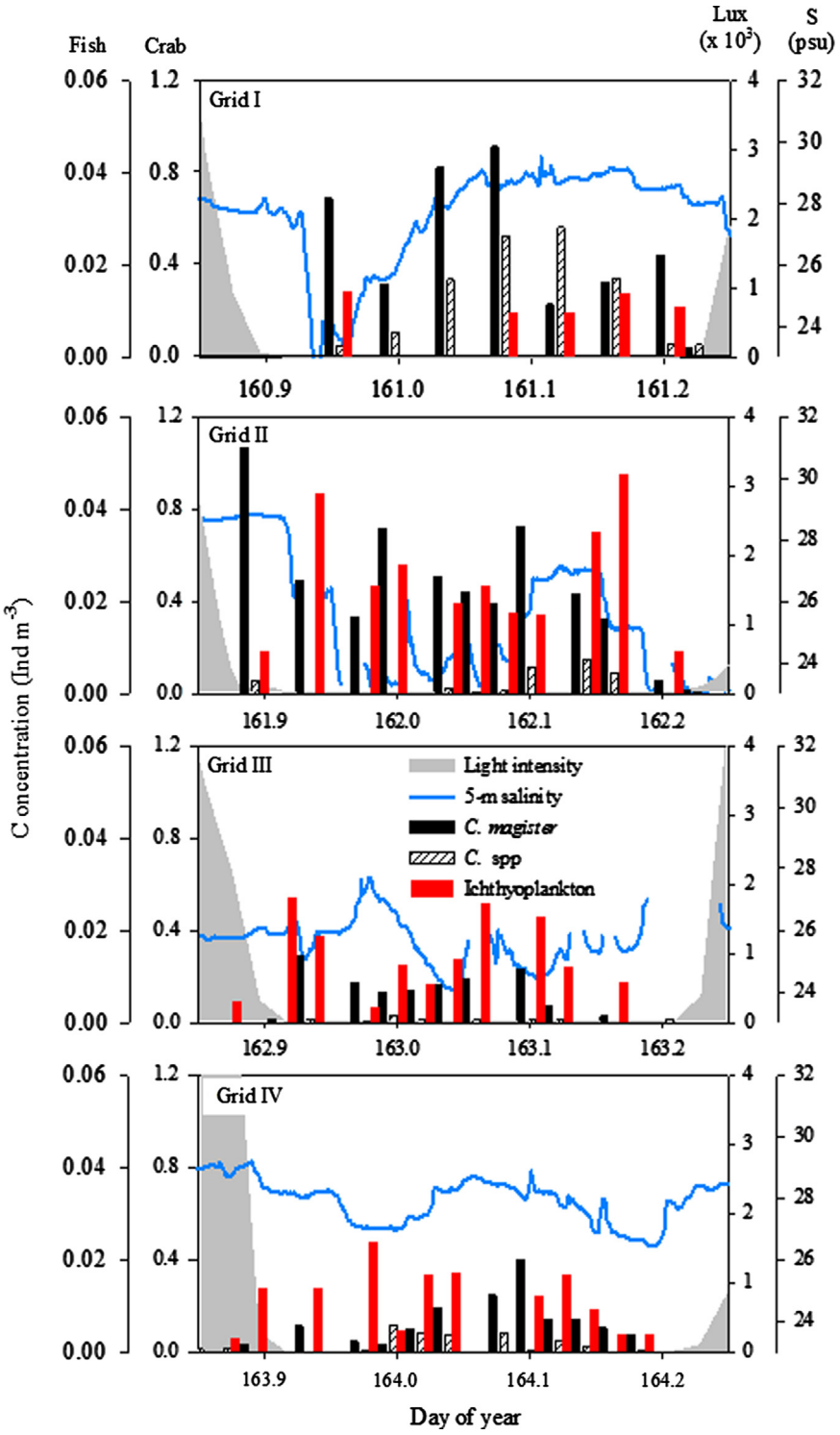

Fig. 4. Time series of *Cancer* crab megalopae (black and white bars), ichthyoplankton (white bars), 5-m salinity (gray line), and light intensity (gray shading) during Grids I–IV.

C. oregonensis/productus decreased 13-fold between Grid I and subsequent surveys (Table 3).

Significantly higher abundances of total fish were sampled along Grid II and the cross-shelf transect than in Grids I and IV (ANOVA; $p=0.04$; Fig. 7). Peak concentration of juvenile rockfishes was found along Grid II, and these concentrations were significantly higher than those found on Grids III, IV, or the alongshore transect ($p=0.04$; Fig. 5). Larval sculpin concentration was higher in the alongshore transect than in any other survey, and the cross-shelf transect had higher sculpin concentrations than Grids III and IV ($p=0.002$; Fig. 5). Concentrations of juvenile ronquils, osmerids, and kelp greenling did not differ over the sampling effort, with the exception of a few surveys with complete absences for specific species (i.e. no ronquils or osmerids at Grid I, and no kelp greenlings at Grid I and the alongshore transect; Fig. 5).

3.8. Relationship to environmental variables

We used a correlation matrix to examine neuston concentration with the physical predictors of light intensity, hours relative to

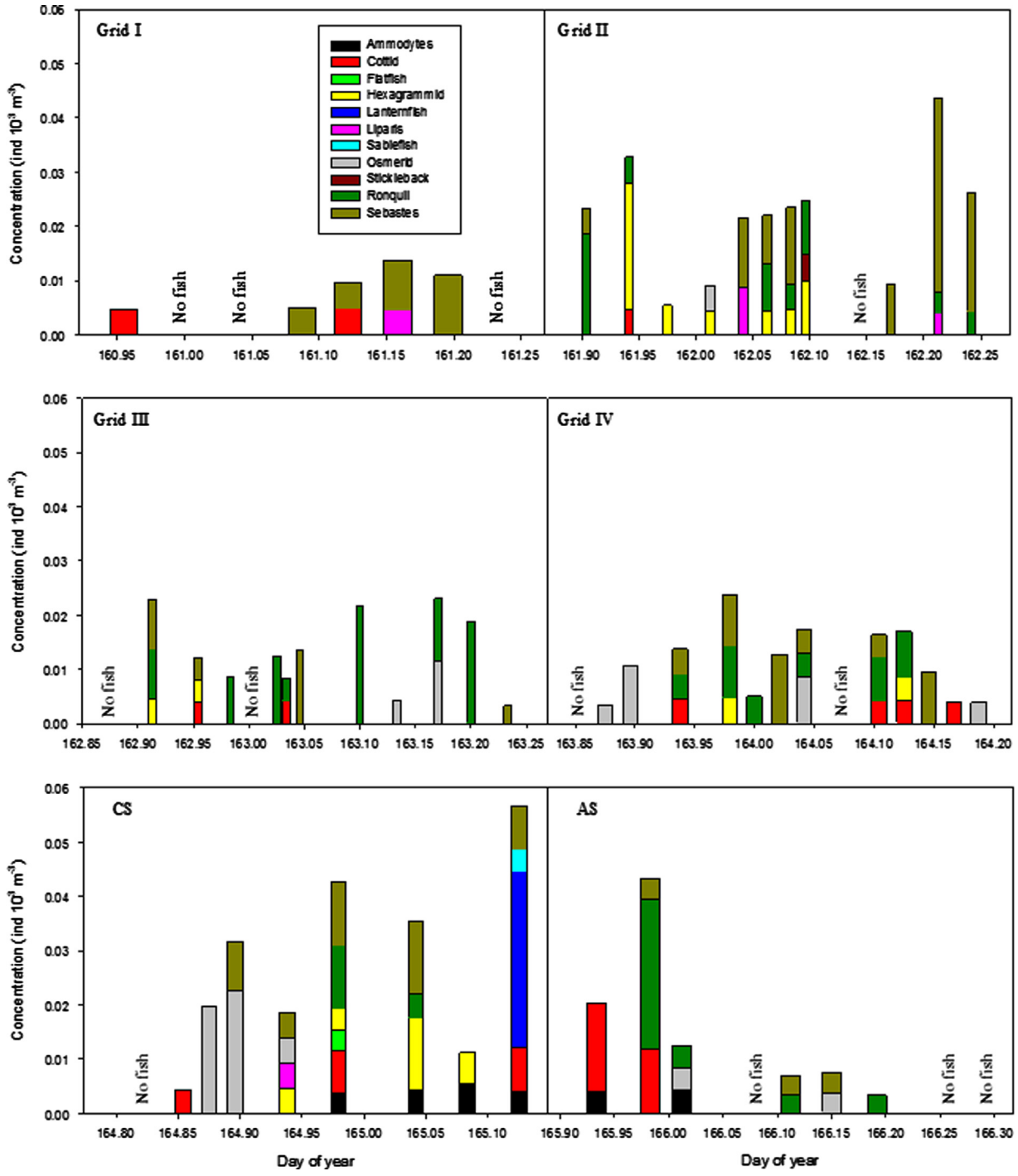

Fig. 5. Time series of fish species concentration sampled from grid (I–IV), and cross-shelf (CS) and along-shore (AS) transects showing changes associated with the seaward advection of plume water.

sunset, temperature, and salinity (Fig. 9; Table 4). For both brachyurans and fish, correlations were moderate to weak, and few tests were significant. In general, *C. magister* megalopae were distributed broadly and were found over the entire range sampled for both temperature (11.4–14.4 °C) and salinity (21.1–31.2) sampled. There was a weak but significant positive correlation with temperature ($r=0.28$) and a significant negative correlation with light intensity ($r=-0.59$). *C. oregonensis/productus* megalopae had a narrower distribution in relation to surface water parameters. Larvae were mostly confined to temperatures between 13 and 14 °C and salinity between 27 and 29. *C. oregonensis/productus* megalopae were significantly correlated with salinity ($r=0.42$), but there were no other significant. For ichthyoplankton, the only significant correlations were those of juvenile rockfishes and ronquils, wherein concentrations were negatively correlated with light intensity (Table 4).

Multivariate statistical analysis of the crab and fish community at each station within the grid indicated that the communities sampled in Grids I and II were significantly different from those in Grids III, IV, and the cross-shelf transect, but were not different from those in the alongshore transect (ANOSIM global $R=0.271$; $p=0.001$; Fig.8).

Environmental data and responses of the dominant neuston concentrations were shown to have significant relationships, and

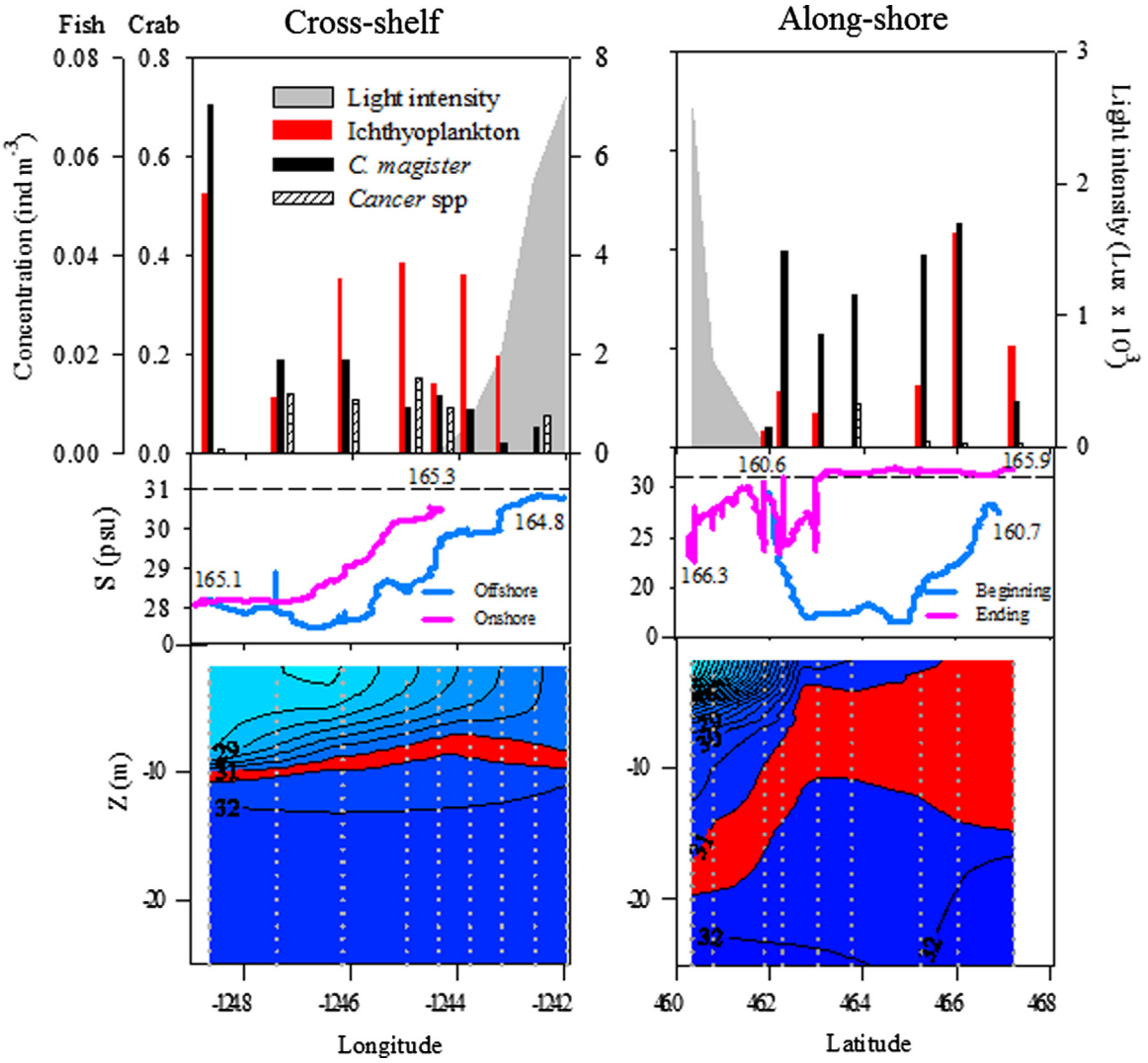

Fig. 6. Cross-shelf (A) and along-shore (B) transect surveys. Upper plots: megalopae and ichthyoplankton concentrations and light intensity. Middle plots: 5-m salinity during outward (blue) and return (pink) legs. Date (day of year format) given for beginning and end of each leg. Dashed line designates salinity of 31; note changes in salinity scale between A and B. Plankton samples were collected during outward (CS transect) and ending (AS transect) surveys, respectively. Lower plots: Vertical salinity during outward (CS transect) and ending (AS transect) legs. CTD casts shown in gray. Isohalines are 0.5; stippled pattern indicates ocean water of salinity 31.0–31.5 (For interpretation of the references to color in this figure legend, the reader is referred to the web version of this article.).

best-fit models were created using non-parametric multiplicative regression analyses (NMPR). For concentration of *C. magister*, the best-fitting model included hours from sunset. Concentration response peaked in catches from the middle of the night, lower concentrations at moderate salinity l (25) and at slack tide (Fig. 9; Table 5). Concentrations of *C. oregonensis/productus* megalopae had the strongest correlations with physical predictors (r^2=0.72): concentrations peaked in response to hours from sunset (with a second peak at midnight), moderate temperatures, and high salinity water. The best-fitting model for *Sebastes* spp. included moderate temperature and low salinity water (Table 5). There was no best-fitting model for *Ronquils jordani*, and the bestfitting model for *H. nudus* was not significant after model evaluation.

We found numerous instances of salinity fluctuations exceeding 0.5/5-min measurement interval, which we interpreted as salinity fronts (Fig. 10). Many frontal zones were sampled in Grids II and III, when the plume was advecting offshore, as well as in the alongshore transect, when we crossed the near-field plume. Fewer salinity gradients exceeding 0.5/5-min interval were found in Grid I, and none were observed while sampling Grid IV or the cross-shelf transect. The northern section of the alongshore transect also lacked detectable fronts. However, correlations of larval crab and fish concentrations (not shown) with the salinity gradient provided little evidence of enhanced concentrations of megalopae or fish juveniles within salinity fronts (Fig.11).

4. Discussion

We hypothesized that the surface distribution of brachyuran larvae and ichthyoplankton would track the dynamics of the Columbia River plume. Ocean conditions in late spring 2010 were affected by a prolonged El Niño event, with protracted downwelling winds and an intense Aleutian low pressure system (Crawford and Robert, 2011; Bjorkstedt et al., 2011). The cruise period coincided with a large Columbia River freshet and also with the seasonal transition to persistent summer upwelling conditions. As a result, our sampling captured a large-scale seaward advection of the far-field Columbia River plume, which was forced by changes in alongshore wind stress. Concurrent neuston sampling for brachyuran larvae and ichthyoplankton revealed varied responses to this advection by early life stages of the dominant

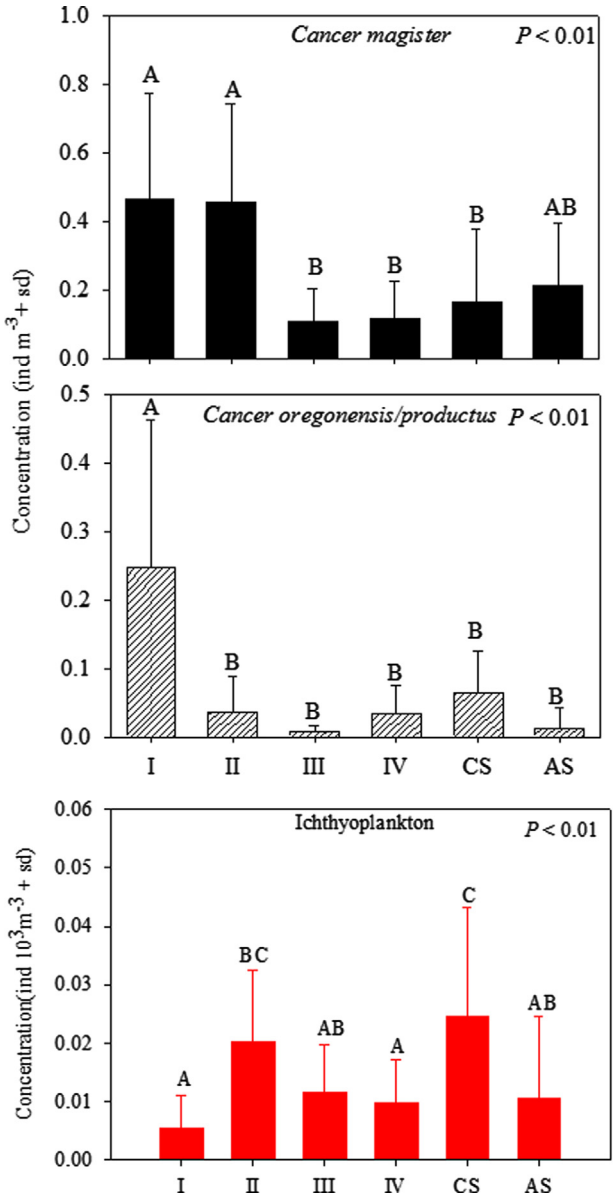

Fig. 7. Mean concentration (standard deviation) and ANOVA results comparing crab larvae and total ichthyoplankton sampled from grid (I–IV), cross-shelf (CS), and along-shore (AS) transects. Letters designate groups not significantly different from each other.

species of crabs and fish. The hypothesis of passive transport was only partially supported, as some planktonic groups maintained a nearshore orientation despite the oceanographic changes that occurred during our study period.

4.1. Plume dynamics

During the first two nights of sampling, there was a northward-trending plume and upwelling-favorable winds were building. Lower-salinity plume water was observed entering the sampling grid from the east. During the subsequent two nights, upwelling wind intensity increased, surface-salinity gradients reversed, and fresher water was advected westward, out of the sampling grid. Average surface salinities first decreased and then increased. On the fifth night, we traced the plume offshore, where we found the lowest salinities at the westernmost station, 60.9 km from shore. The final night, we measured high salinity and upwelling north and the new plume to the south. These observations were

Table 3
Estimated total abundance (individuals × 10^6) of megalopae in nighttime surface waters during each grid survey, standardized to a 100 km^2 area.

Species	Grid I	Grid II	Grid III	Grid IV
Cancer magister	13.3	13.0	2.7	2.2
Cancer oregonensis/productus	6.5	0.6	0.3	0.7

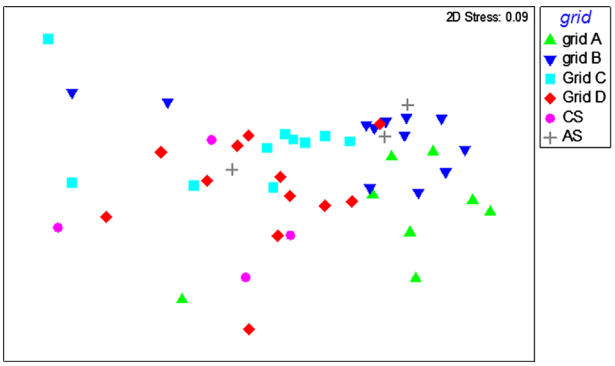

Fig. 8. Non-metric multidimensional scaling (MDS) ordination plot of the community composition of crab megalopae and fish larvae for grid stations only.

consistent with predictions of seaward advection for northward-trending plumes by the surface Ekman transport (Hickey et al., 2005, 2009).

Surface salinity measured during the westward and eastward legs of the cross-shelf transect provided an estimate of the offshore advection rate of plume-influenced water. The 30.5 isohaline moved ~9.6 km offshore in 9.5 h, yielding a velocity of 0.28 m s^{-1} (24.2 km d^{-1}). In comparison, the wind-induced cross-shelf plume velocities derived by Hickey et al. (2005) ranged 0.12–0.17 m s^{-1} (10–15 km d^{-1}) at buoys deployed off the mid-Washington coast, and Peterson and Peterson (2009) tracked semidiurnal tidal movement of the plume at 0.38 m s^{-1} (32.8 km d^{-1}) offshore from the Columbia River. These data indicate that both wind and tidal forcing can rapidly propel the buoyant plume seaward.

As discerned by the relatively constant position of the 31 isohaline near the 10-m depth, coastal upwelling was not evident during most of the cruise, despite upwelling-favorable wind stress (Fig. 6A). Only during the final night (day 6), when we made the alongshore transect, did upwelled ocean water replace the plume. Replacement of plume water by upwelled water was determined by upwardly sloped isohalines and surface water approaching a salinity of 31 (Fig. 6B). In contrast, we found the near-field plume directed south and capping higher-salinity water in the southern section of the alongshore transect.

Hickey et al. (2005) found a lag time of several days in the arrival of upwelled water after initiation of upwelling winds. Roegner et al. (2002) surveyed a large grid pattern off Willapa and Grays Harbor during late May 1999, before and after a wind-induced change in plume orientation. During that study, upwelled water was well established across the shelf within 4 days of the switch to upwelling winds, and a significant phytoplankton bloom was produced. The magnitude of Columbia River flow volume was only ~7700 m^3 s^{-1} during the cruise of May 1999 versus ~11000 m^3 s^{-1} during our cruise in 2010. Thus, a higher cumulative wind stress was likely required to move the larger plume and initiate upwelling during the present cruise. Our study occurred during the actual seaward advection phase of the plume, when the plume was between the states sampled by Roegner et al. (2002, 2003).

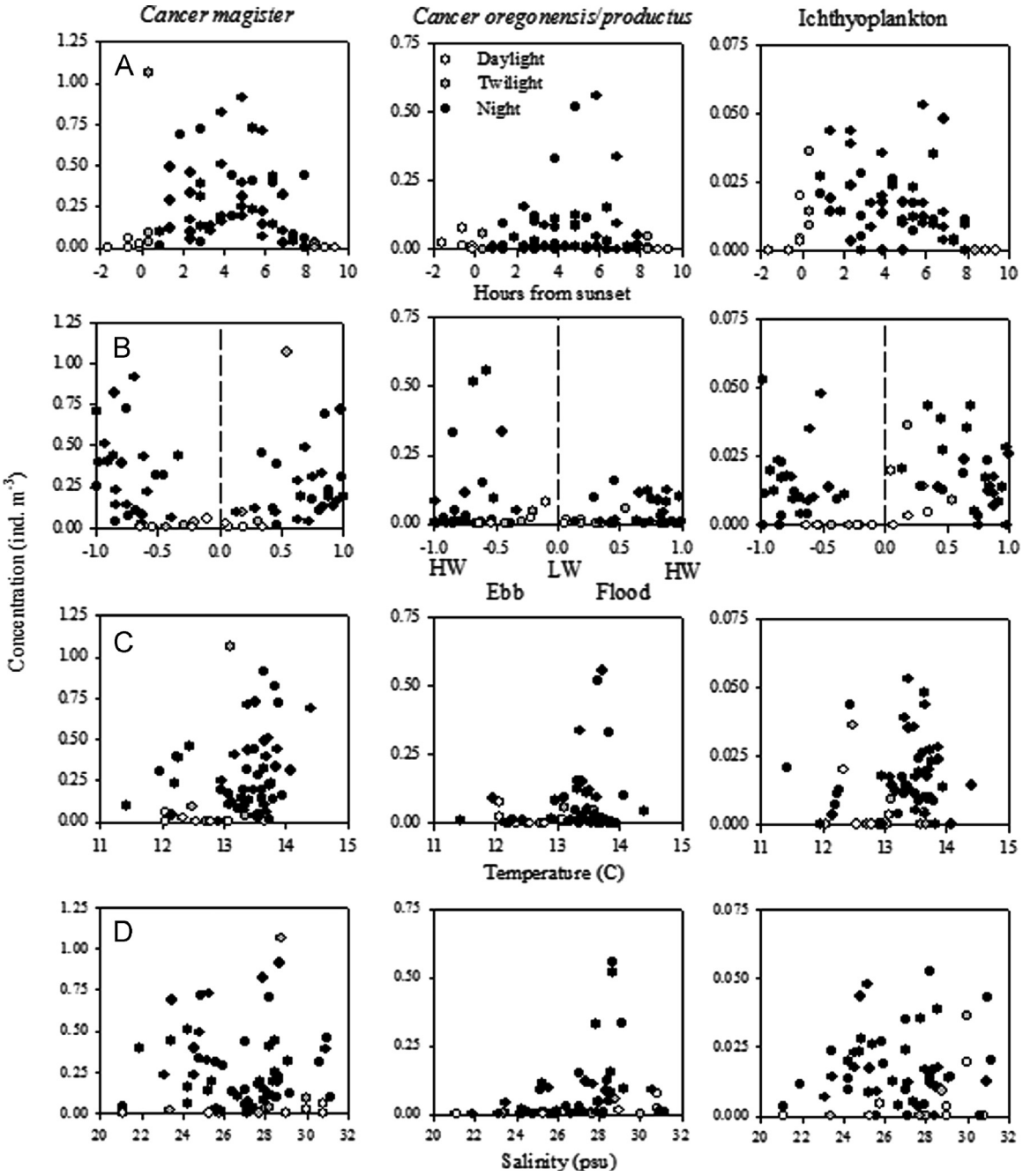

Fig. 9. Scatter plots of *Cancer* crab (individuals m^{-3}) and ichthyoplankton (10^3 individuals m^{-3}) concentrations by (A) hours from sunset; (B) stage of tide (HW = high water, LW = low water); (C) temperature and (D) salinity. Shade of symbols codes for light level to indicate daylight (white), twilight (gray) and nighttime (black) periods.

Table 4
Correlation matrix for brachyuran larvae and ichthyoplankton with environmental variables of light intensity, hours from sundown, temperature, and salinity.

Species	Light intensity (lux)	Hours from sundown	Temp (°C)	Salinity (psu)	Stage of tide
C. magister	**−0.59**	0.02	**0.28**	−0.02	0.06
Cancer spp.	−0.03	0.10	0.14	**0.42**	−0.04
H. oregonensis	−0.18	0.07	−0.06	**0.31**	−0.13
R. jordani	**−0.26**	0.01	0.09	−0.13	0.07
Sebastes spp.	**−0.27**	0.15	0.18	−0.06	−0.08

Bold values indicate significant difference ($p < 0.05$). *Cancer spp: Cancer oregonensis/productus.*

4.2. Crab dynamics

Response of megalopae to the large advective event that occurred during our sampling cruises was varied. *C. oregonensis/productus* megalopae were most abundant during the first sample period and appeared to be swept offshore with the plume water, in support of the hypothesis. Concentrations inshore remained lower, even when high-salinity water returned to the nearshore surface. Concentrations of *C. magister* megalopae were also reduced in the grid after passage of the plume, but many megalopae were retained in the nearshore sampling area, and concentrations were high inshore in both plume and higher-salinity water, possibly due to swimming

Table 5
Best-fit non-parametric multiplicative regression (NPMR) model results for brachyuran larvae and ichthyoplankton with environmental variables: hours from sundown, temperature (°C), salinity, and stage of tide.

Species	Best-fitting model environmental variables	Cross-validated r^2	p-value
C. magister	Sundown, salinity, stage of tide	0.36	0.040
Cancer spp.	Sundown, temp, salinity	0.72	0.001
H. oregonensis	Sundown, temp, stage of tide	0.20	N.S.
R. jordani	No valid model	–	–
Sebastes spp.	Temp, salinity	0.26	0.020

Cancer spp: Cancer oregonensis/productus.
N.S.; not significant.

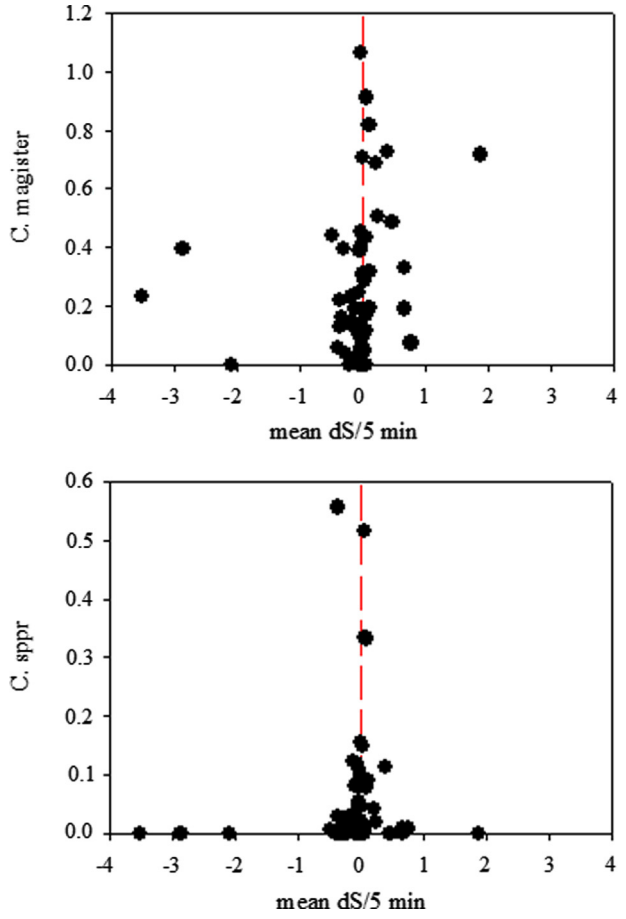

Fig. 10. Scatter plots of *Cancer* crab megalopae concentration (individuals m^{-3}) versus salinity gradient (dS/dt).

behaviors. The third crab species we measured, *Hemigrapsus nudus*, also followed this pattern, although its overall concentrations were low and not significantly different between samples. These results demonstrate larval populations persisted at nearshore settlement sites during active offshore advection of the plume, contrary to predictions of the hypothesis.

Similar results were found by Roegner et al. (2003) during surveys that sampled downwelling conditions with a coastal-oriented plume and subsequent upwelling conditions with an offshore-oriented plume. In that study, *C. magister* concentrations were contiguous under both wind conditions ($\gamma > 3.0$), but megalopae were present at approximately equal mean concentrations in both plume and newly upwelled water. However, other larval crab and barnacle species exhibited strong responses to the advection event by change in either abundance (crabs) or position (barnacles; Roegner et al., 2002). Recent studies from a strong upwelling zone in the southern CCS also show behaviorally mediated retention of these species in the nearshore zone, despite seaward advective forces (Morgan et al., 2009b, 2012; Shanks, 2009). These data suggest varied and perhaps species-specific responses of larvae to physical forcing.

Of the three species of brachyuran crab megalopae were found in the neuston of plume water, *C. magister* dominated the catch during all sample periods. The frequency of occurrence of *C. magister* in both grid and transect surveys was extensive (FO=0.92), and was higher than those found in many previous studies (e.g. Booth et al., 1985; Brodeur et al., 1987; Roegner et al., 2003; Reese et al., 2005) but similar to that found by Shenker (1988). In the grid surveys, frequency of occurrence was indicative of larval patch size, which likely exceeded the area sampled. Previous estimates of *C. magister* aggregation have found contiguous distributions that ranged from 2 to 5 km (Booth et al., 1985; Shenker, 1988; Roegner et al., 2003), but in our study patches exceeded 13 km (the transect length). The relatively low skewedness of the crab concentration measured indicated an even distribution within the grid area surveyed. At the highest concentration, we estimated an abundance of over 13×10^6 *C. magister* individuals per 100 km^2 of sea surface.

Mean *C. magister* concentration ($C=0.24 \pm 0.25$) was higher than those measured in the northern and central CCS by Roegner et al. (2003); $C=0.04 \pm 0.08$ or Reese et al. (2005); $C=0.14 \pm 0.29$, but lower than those measured within frontal zones by Lough (1976); $C=8$, Shenker (1988); $C=24$, Eggleston et al. (1998; $C=10.7 \pm 2.6$), or Morgan et al. (2005); C=3.0. Correlations of larval crab concentration with the horizontal salinity gradient in our study provided little evidence of accumulations of megalopae within salinity fronts (Fig.10), a finding in contrast with the studies cited above. These previous high catches were often made by directed sampling along convergence zones, and merely intersecting the relatively narrow (2–4 m) surface fronts as we did will not necessarily lead to a large enhancement in catch. Alternatively, salinity measurements at 5 m may not represent the position or strength of surface convergence zones.

Less information is available for distributions of *C. oregonensis/productus* or *Hemigrapsus nudus* in the CCS. During our study, *C. oregonensis/productus* in the neuston had a wider distribution but similar mean concentration compared to the survey by Reese et al. (2005), who sampled non-plume water of the central CCS during June 2000 (FO=0.71 versus 0.27; $C=0.06 \pm 0.11$ versus 0.11 ± 0.25). *H. nudus* was found infrequently by Reese et al. (2005), and Roegner et al. (2003) did not report high concentrations or frequencies of occurrence for *C. oregonensis/productus* or *H. nudus* off Willapa Bay in late May 1999. However, mean concentrations of kelp (*Pugettia producta*) and hermit crab megalopae (*Pagurus* spp.) were relatively high in newly upwelled water ($C=0.11 \pm 0.24$ and 0.12 ± 0.42, respectively), and were rare or absent within the plume during that study.

Light was the best predictor of *C. magister* abundance (a negative association). However, most of the 64 net tows were made during hours of darkness (~8.5 h duration during the study period), and only 18% were made during twilight or higher light intensities. Dungeness crab larvae can be present in the neuston during both night and day, but abundances are generally higher at night. Shenker (1988) sampled the neuston along the Newport Hydroline (44.67°N) during day and night and found FOs of 0.71 during day versus 0.94 during night. In the same region as the present study, Roegner et al. (2003) caught significantly more megalopae in the neuston at night, but larvae were also present at high light intensities during the day. Several studies have noted high abundance during crepuscular periods (Booth et al., 1985; Jamieson and Phillips, 1988; Hobbs and Botsford, 1992), which we did not observe. We found *C. magister* larvae at light levels up to 5511 lx and in four

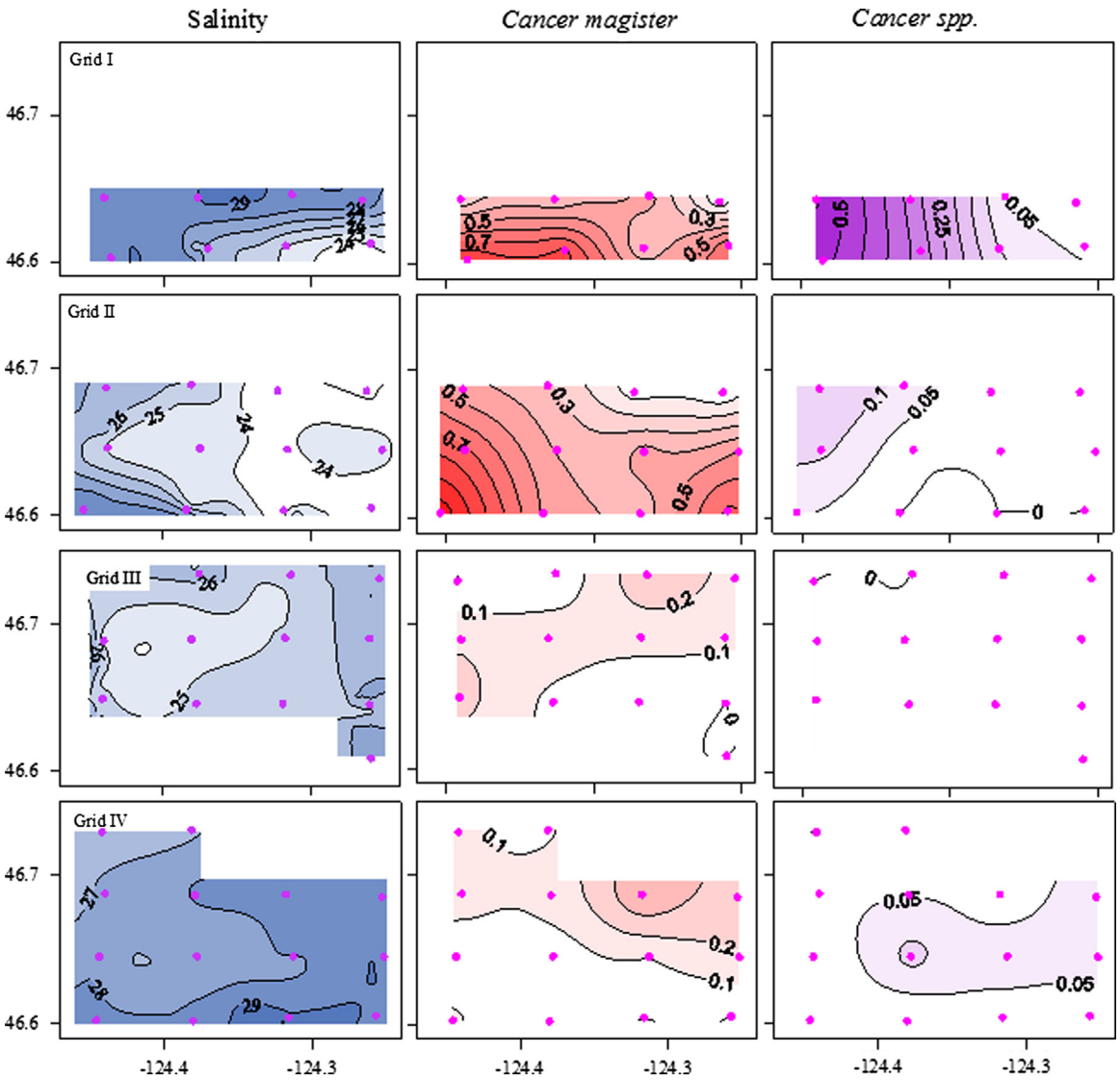

Fig. 11. Surface plots of salinity and the concentrations of *Cancer magister* and *Cancer productus/oregonensis* megalopae in Grids I–IV. Contour isopleths are 1.0 for salinity, 0.1 ind m^{-3} for *C. magister*, and 0.05 ind m^{-3} for *C. productus/oregonensis*.

of 11 hauls made at intensities >100 lx. *C. oregonensis/productus* larvae were found at the four highest light intensities we sampled (3961–7233 lx), but were absent during other morning or evening periods, and their concentration was not correlated with light intensity.

Another factor to consider is the settlement behavior of megalopae. In the PNW, *C. magister* megalopae settle from the plankton to estuaries and the nearshore zone (depths <100 m) from March through November, with peak recruitment to estuaries generally occurring in May or June (Roegner et al., 2003, 2007). Thus, our cruise coincided with the location and timing of crab settlement. Planktotrophic invertebrate larvae must feed to acquire the energy reserves that fuel metamorphosis to benthic life. Larvae that achieve this state are known as "competent." In a small onboard competency experiment with *C. magister*, we placed eleven individual *C. magister* megalopae into small containers at a salinity of 28 and observed them for metamorphosis to the first benthic stage. We found nine of the 11 megalopae settled and metamorphosed within 36 h. These informal observations indicate megalopae were physiologically competent to settle from the water column and complete transition to the benthic life phase. Thus, an alternative explanation for the decrease in surface concentration is that larvae had avoided offshore advection by settling to the substrate, possibly induced by cues from changing ocean conditions (upwelling).

4.3. Fish dynamics

Neustonic fish sampled in the NCC during a late-spring downwelling event were characteristically well-developed, with several species of a size typically reached prior to juvenile settlement. The presence of fish at this stage is associated with the onset of summer upwelling conditions (Shenker 1988; Doyle 1992a; Larson et al., 1994). As observed during sampling of crab larvae along the cross-shelf transect, there was a significant decrease in abundance and increase in offshore movement of ichthyoplankton with the onset of upwelling, in support of the hypothesis. However, as with crab larvae, we also found evidence of nearshore retention for several species.

The juvenile rockfish sampled in 2010 were identified mainly as either widow or yellowtail rockfish and were late-stage juveniles (mean size 53.6 mm). Rockfishes caught had relatively high frequency of occurrence (0.40) and abundance (4.2×10^3 m^{-3}) in surface inshore waters (9–14 km from shore). This finding

was relevant to those of Norton (1987), who observed a positive relationship between first-year survival of widow rockfish and El Niño ocean conditions with strong Aleutian low pressure systems. Both these climatic conditions tend to increase the onshore transport of surface waters through stronger-than-usual downwelling events.

Large juvenile rockfish have been shown to move inshore prior to settlement and to use swimming behaviors such as vertical migration to maintain an inshore position, even during upwelling events (Larson et al., 1994). During our study, the high abundance of large-sized juvenile rockfishes captured close to shore suggests the potential for settlement and high recruitment success (Larson et al., 1994). Shenker (1988) caught juvenile rockfish in higher abundance in May than during our study period ($C=8.99$), yet his study included stations much further from shore (90 km), where juvenile rockfish can be found in high concentration (Auth, 2009). The juvenile rockfishes that we caught in early June 2010 were possibly products of early winter spawning, as noted by Richardson (1973). Considering that we sampled only one larval rockfish during our entire effort, it is possible that we observed just the start of a process of larval rockfish advection from offshore habitats to coastal waters (Shenker, 1988; Auth, 2009).

The second most frequently sampled ichthyoplankton was juvenile ronquil, which is considered to be a persistent species that is caught both before the onset of upwelling and during the upwelling season (Shenker, 1988). The frequency of occurrence, abundance, and size of ronquil we sampled was similar to earlier studies of neustonic ichthyoplankton (Shenker, 1988; Doyle, 1992a).

Our catch of juvenile hexagrammids was also similar to those of two previous studies (Shenker, 1988; Doyle, 1992b), but our fish were much larger, especially considering the size of net used during our study. In Shenker's study, large hexagrammids were able to avoid being caught in his smaller neuston net (similar to the one we used). However, a larger neustonic "trawl" net, which was towed simultaneously, caught large hexagrammids frequently in June (51.2 mm; Shenker 1988). Juvenile kelp greenlings are thought to be present in the neuston prior to the onset of upwelling and are considered obligate residents of surface waters in both nearshore and offshore habitats (Richardson and Pearcy, 1977; Shenker, 1988).

Pacific sandlance were not caught until the last two days of our sampling effort and were found either at the outermost stations of the cross-shelf transect or at the innermost stations of the sampling grid. Once again, Pacific sandlance individuals were large in size relative to those caught during other studies, but catches were lower in frequency and abundance. In contrast, we sampled osmerid larvae at a higher frequency and different time of year than seen in other neustonic studies (Shenker, 1988; Doyle 1992a), although Richardson and Pearcy (1977) also found peak catches of osmerids in June using a surface-oriented (0–10 m net depth) mid-water trawl. Juvenile osmerids are common within the Columbia River estuary during May and June.

Notably, larval and juvenile sculpins and flatfish were sampled infrequently or not at all, even though Brodeur (1989) has shown them to be common neustonic fish in the study area. We also did not encounter any larval anchovy (*Engraulis mordax*), a species known to spawn in the Columbia River plume (Richardson, 1973) and often caught there (Parnel et al., 2008). Anchovy may have had a later spawning due to the delayed upwelling conditions in the CCS during 2010.

In terms of life-history variation (based on size), the smallest larvae we collected were all from the last two days of sampling. This may have indicated larval advection of nearshore taxa into our sampling area with recently upwelled water. Most small fish were larval cottids that have pelagic larvae found over a broad range of nearshore waters, and may have originated from a local spawning source. The only larval *Sebastes* spp. caught was on the last day of sampling, when we found evidence of recently upwelled ocean water. This may have indicated the start of subsurface onshore advection of *Sebastes* spp. larvae. Finally, sablefish (*Anoplopoma fimbria*) and myctophids, fish considered part of the offshore assemblage (Auth and Brodeur, 2006), were caught only at the westernmost station of the cross-shelf transect.

4.4. Synthesis

The Columbia River plume forms a unique habitat in the CCS due to its steep biophysiochemical gradients. Plume structure and position are dynamically controlled by variations in wind stress, river flow, and tidal forcing (Hickey et al., 2010). Few organisms produce planktonic larvae that can undergo development and dispersal entirely in the low-salinity water of the plume. Even the northern anchovy *E. mordax*, which spawns in the plume and is among the most plume-dependent species, produces eggs and larvae that are often found outside the plume (Brodeur et al., 1985, Auth and Brodeur, 2006). Thus most organisms observed in the neuston samples must have arrived there from advective mixing and/or vertical migration.

Coastal distribution of late-stage larval crustaceans and juvenile fishes is a function of multiple factors. These include larval release time, duration of planktonic development, behaviorally mediated vertical position, and physical advective forces such as upwelling and plume dynamics (Dempster et al., 1997; Reiss and McConaugha, 1999; Shanks, 2009). Most of the species we observed had relatively long larval durations (>1 mo), spawned in winter during downwelling-dominant conditions, and recruited after the spring transition and initiation of upwelling (Shanks and Eckert, 2005; Shanks and Roegner, 2007; Shanks, 2009). These dispersal traits may take advantage of large scale oceanographic processes in the CCS to facilitate the return of larvae from pelagic rearing areas to favorable benthic habitats (Sinclair, 1988; Shanks and Eckert, 2005).

Although, we have shown that an episodic advective event can clearly influence plankton distribution, other recent studies in the CCS and elsewhere have demonstrated that larvae can maintain preferred locations during development via behavioral adaption, even against strong advection events (Shanks et al. 2002; Shanks and Brink, 2005; Shanks and Shearman, 2009; Morgan et al., 2009a, b; 2012). It is clear that with swimming speeds of 0.08 m s^{-1} (Fernandez et al., 1994) and capture depths exceeding 100 m (Jamieson and Phillips, 1993), the large *C. magister* (5–7 mm carapace) is capable of significant movements. *C. oregonensis/productus* megalopae are smaller (2–3 mm) and may be less competent swimmers, but they are certainly more adept swimmers than larvae with ciliary propulsion (Roegner et al., 2003). Migration of fish and crab larvae into water masses of different current regimes is a likely mechanism for larvae to influence their dispersal.

The observation of variability in the response of crab megalopae to light suggests a means for the varied responses observed in the plankton distributions. Larvae that follow a regular diurnal migration period would tend to disperse together, and in the case of a large advective event such as the one we measured, would be transported offshore in the surface layer. Our observed distributions of *C. oregonensis/productus* fit this pattern. In contrast, larvae that spend more time away from the surface Ekman layer would have reduced movement offshore during upwelling, and increased inshore movement in the bottom return flow (Shanks, 1995; Morgan et al., 2009b). *C. magister* megalopae that were retained near shore may have followed this pattern.

The fish we sampled retained a common species composition during the shift from downwelling to upwelling conditions, but there were changes in both fish size and abundance during the last

several days of the cruise. Oceanographic changes due to the shift in the CCS from downwelling to upwelling winds may be a cue for settlement in some neustonic fish to avoid being advected offshore in wind-driven (and plume-driven) surface water (Shenker, 1988).

Advective transport of the Columbia River plume in nearshore waters has significant effects on the oceanography of the Northern California Current System. On episodic time scales, upwelling–downwelling cycles control plume direction and affect the biophysical processes on the Washington and Oregon shelves (Hickey et al., 2010). During this study, we captured the transition from a series of cyclic wind patterns during spring to a period of persistent upwelling during summer. The response of planktonic crab larvae and ichthyoplankton to this large-scale advection varied by species, with larger and more vagile fish exhibiting less evidence of passive transport than smaller crab larvae. Although fish and crab larvae were advected offshore with the plume, some species, notably *C. magister* megalopae, maintained high concentrations nearshore in newly upwelled water after passage of the plume offshore. These results show a conservation of larvae in favorable settlement habitat in the presence of strong advective forcing.

Acknowledgments

We sincerely thank scientists Sarikka Attoe, Caren Barceló, and Amanda Gladics, and electronic technicians Manuel Calderon and Phil White for help with the sampling. Toby Auth, JoAnne Butzerin, Jennifer Fisher, and Kurt Fresh provided very helpful comments on an earlier version of the manuscript. Funding for this research was provided by Bonneville Power Administration and the National Marine Fisheries Service.

References

Auth, T.D., 2009. Importance of far-offshore sampling in evaluating the ichthyoplankton community in the northern California Current. CalCOFI Reports 50, 107–117.

Auth, T.D., Brodeur, R.D., 2006. Distribution and community structure of ichthyoplankton off the Oregon coast, USA, in 2000 and 2002. Marine Ecology Progress Series 319, 199–213.

Banas, N.S., Hickey, B.M., Newton, J.A., Reusink, J.L., 2007. Tidal exchange, bivalve grazing, and patterns of primary production in Willapa Bay, Washington, USA. Marine Ecology Progress Series 341, 123–139.

Bjorkstedt, E.P., Goericke, R., McClatchie, S., Weber, E., Watson, W., Lo, N., Peterson, B., Emmett, R., Brodeur, R., 2011. State of the California Current 2010–2011. Regionally variable responses to a strong (but fleeting?) La Niña. CalCOFI Reports 52, 36–58.

Booth, J., Phillips, A., Jamieson, G.S., 1985. Fine scale spatial distribution of *Cancer magister* megalopae and its relevance to sampling methodology. In: Melteff, B.R (Ed.), Proceedings of the Symposium on Dungeness Crab Biology and Management. Alaska Sea Grant Report, 85–3. University of Alaska, Alaska, pp. 273–286.

Brodeur, R.D., 1989. Neustonic feeding by juvenile salmonids in coastal waters of the Northeast Pacific. Canadian Journal of Zoology 67, 1995–2007.

Brodeur, R.D., Gadomski, D.M., Pearcy, W.G., Batchelder, H.P., Miller, C.B., 1985. Abundance and distribution of ichthyoplankton in the upwelling zone off Oregon during anomalous El Niño conditions. Estuarine, Coastal and Shelf Science 21, 365–378.

Brodeur, R.D., Pearcy, W.G., Mundy, B.C., Wisseman, R.W., 1987. The neustonic fauna in coastal waters of the Northeast Pacific: abundance, distribution and utilization by juvenile salmonids. Oregon State University Sea Grant Pub. ORESU-TU-87-001, 61 pp.

Clarke, K.R., 1993. Non-parametric multivariate analysis of changes in community structure. Australian Journal of Ecology 18, 117–143.

Clarke, K.R., Gorley, R.N., 2006. PRIMER v6, User Manual/Tutorial. PRIMER-E, Plymouth.

Crawford, W., Robert, M., 2011. The State of the Northeast Pacific in 201019. PICES Press 38–40.

CRDART (Columbia River Data Access in Real Time), 1995. Online interactive database. Available from ⟨www.cbr.washington.edu/dart/dart.html⟩ (May 2012).

Dempster, T., Gibbs, M.T., Rissik, D., Suthers, I.M., 1997. Beyond hydrography: daily ichthyoplankton variability and short term oceanographic events on the Sydney continental shelf. Continental Shelf Research 17, 1461–1481.

De Robertis, A., Morgan, C.A., Schabetsberger, R.A., Zabel, R.W., Brodeur, R.D., Emmett, R.L., Knight, C.M., Krutzikowsky, G.K., Casillas, E., 2005. Columbia River plume fronts. II. Distribution, abundance, and feeding ecology of juvenile salmon. Marine Ecology Progress Series 299, 33–44.

Doyle, M.J., 1992a. Neustonic ichthyoplankton in the northern region of the California Current System. CalCOFI Reports 33, 141–161.

Doyle, M.J., 1992b. Patterns in Distribution and Abundance of Ichthyoplankton off Washington, Oregon, and Northern California (1980–1987). U.S. Department of Commerce, National Marine Fisheries Service, Northwest and Alaska Fisheries Center Processed Reports, 92–14, 344 pp.

Eggleston, D.B., Armstrong, D.A., Elis, W.E., Patton, W.S., 1998. Estuarine fronts as conduits for larval transport, hydrodynamics and spatial distribution of Dungeness crab postlarvae. Marine Ecology Progress Series 164, 73–82.

Emmett, R.L., Krutzikowsky, G.K., Bentley, P., 2006. Abundance and distribution of pelagic piscivorous fishes in the Columbia River plume during spring/early summer 1998–2003: relationship to oceanographic conditions, forage fishes, and juvenile salmonids. Progress in Oceanography 68, 1–26.

Fernandez, M., Iribarne, O.O., Armstrong, D.A., 1994. Swimming behavior of Dungeness crab, *Cancer magister* Dana, megalopae in still and moving water. Estuaries 17, 271–275.

Hickey, B.M., Banas, N.S., 2003. Oceanography of the US Pacific Northwest coastal ocean and estuaries with application to coastal ecology. Estuaries 26, 1010–1031.

Hickey, B.M., Pietrafesa, L.J., Jay, D.A., Boicourt, W.C., 1998. The Columbia River plume study, subtidal variability in the velocity and salinity field. Journal of Geophysical Research 103, 1033910368.

Hickey, B.M., Geier, S.L., Kache, N.B., MacFadyen, A., 2005. A bi-directional river plume, the Columbia in summer. Continental Shelf Research 25, 1631–1656.

Hickey, B.M., McCabe, R., Geier, S., Dever, E., Kachel, N., 2009. Three interacting river plumes in the northern California Current System. Journal of Geophysical Research 114, C00B03, http://dx.doi.org/10.1029/2008JC004907.

Hickey, B.M., Kudela, R.M., Nash, J., Bruland, K., Peterson, W., 2010. and 16 others, 2010. River influences on shelf ecosystems: introduction and synthesis. Journal of Geophysical Research 115, C00B17, http://dx.doi.org/10.1029/2009JC5452.

Hill, A.E., 1995. The kinematical principles governing horizontal transport induced by vertical migration in tidal flows. Journal of the Marine Biological Association of the United Kingdom 75, 3–13.

Hobbs, R.C., Botsford, L.W., 1992. Diel vertical migration and timing of metamorphosis of larvae of the Dungeness crab *Cancer magister*. Marine Biology 112, 417–428.

Horner-Devine, A.R., Jay, D.A., Orton, P.M., Spahn, E., 2009. A conceptual model of the strongly tidal Columbia River plume. Journal of Marine Systems 78, 460–475.

Jamieson, G.S., Phillips, A.C., 1988. Occurrence of *Cancer* crab (*Cancer magister* and *C. oregonensis*) megalopae off the west coast of Vancouver Island, British Columbia. Fishery Bulletin 86, 525–542.

Jamieson, G.S., Phillips, A.C., 1993. Megalopal spatial distribution and stock separation in Dungeness crab (*Cancer magister*). Canadian Journal of Fisheries and Aquatic Sciences 50, 416–429.

Larson, R.J., Lenarz, W.H., Ralston, S.R., 1994. The distribution of pelagic juvenile rockfish of the genus *Sebastes* in the upwelling region off central California. CALCOFI Reports 35, 175–221.

Lough, R.G., 1976. Larval dynamics of the Dungeness crab, *Cancer magister*, off the central Oregon coast. Fishery Bulletin 74, 353–375.

McCune, B., Mefford, M.J., 2009. HyperNiche, Version 2.0. MjM Software. Gleneden Beach, Oregon.

Morgan, C.A., De Robertis, A., Zabel, R.W., 2005. Columbia River plume fronts. I. Hydrography, zooplankton distribution, and community composition. Marine Ecology Progress Series 299, 19–31.

Morgan, S.G., Fisher, J.L., Mace, A.J., 2009a. Larval recruitment in an area of strong, persistent upwelling and recruitment limitation. Marine Ecology Progress Series 394, 79–99.

Morgan, S.G., Fisher, J.L., Miller, S.H., McAfee, S.T., Largier, J.L., 2009b. Nearshore larval retention in a region of strong upwelling and recruitment limitation. Ecology 90, 3489–3502.

Morgan, S.G., Fisher, J.L., McAfee, S.T., Largier, J.L., Halle, C.M., 2012. Limited recruitment during relaxation events: larval advection and behavior in an upwelling system. Limnology and Oceanography 57, 457–470.

Norton, J. 1987. Ocean climate influences on groundfish recruitment in the California Current. In: Proceedings of the International Rockfish Symposium, Anchorage, Alaska, AK Sea Grant Report 87–2, University of Alaska, Anchorage. pp. 73–99.

Parnel, M.M., Emmett, R.L., Brodeur, R.D., 2008. Ichthyoplankton community in the Columbia River plume off Oregon: effects of fluctuating oceanographic conditions. Fishery Bulletin 106, 161–173.

Peterson, J.O., Peterson, W.T., 2008. Influence of the Columbia River plume (USA) on the vertical and horizontal distribution of mesozooplankton over the Washington and Oregon shelf. ICES Journal of Marine Science 65, 477–483.

Peterson, J.O., Peterson, W.T., 2009. Influence of the Columbia River plume on cross-shelf transport of zooplankton. Journal of Geophysical Research 114, C00B10, http://dx.doi.org/10.1029/2008JC004965.

Queiroga, H., Blanton, J., 2005. Interactions between behavior and physical forcing in the control of horizontal transport of decapod crustacean larvae. In: Southward, A.J., Tyler, P.A., Young, C.M., Fuiman, L.A. (Eds.), Advances in Marine Biology, vol. 4. Elsevier Academic, San Diego, pp. 118–169.

Reese, D.C., Miller, T.W., Brodeur., R.D., 2005. Community structure of near surface zooplankton in the northern California Current in relation to oceanographic conditions. Deep-Sea Resarch II 52, 29–50.

Reiss, C.S., McConaugha, J.R., 1999. Cross-frontal transport and distribution of ichthyoplankton associated with Chesapeake Bay plume dynamics. Continental Shelf Research 19, 151–170.
Richardson, S.L., 1973. Abundance and distribution of larval fishes in waters off Oregon, May–October 1969, with special emphasis on the northern anchovy *Engraulis mordax*. Fishery Bulletin 71, 697–711.
Richardson, S.L., Pearcy, W.G., 1977. Coastal and oceanic fish larvae in an area of upwelling off Yaquina Bay, Oregon. Fishery Bulletin 75, 125–145.
Roegner, G.C., Armstrong, D.A., Hickey, B.M., Shanks, A.L., 2003. Ocean distribution of Dungeness crab megalopae and recruitment patterns to estuaries in southern Washington State. Estuaries 26, 1058–1070.
Roegner, G.C., Armstrong, D.A., Shanks, A.L., 2007. Wind and tidal influences on crab recruitment to an Oregon estuary. Marine Ecology Progress Series 351, 177–188.
Roegner, G.C., Hickey, B.M., Newton, J.N., Shanks, A.L, Armstrong, D.A., 2002. Wind-induced plume and bloom intrusions into Willapa Bay, Washington. Limnology and Oceanography 47, 1033–1042.
Roughan, M., Mace, A.J., Largier, J.L., Morgan, S.G., Fisher, J.L., Carter, M.L., 2005. Subsurface recirculation and larval retention in the lee of a small headland. A variation on the upwelling shadow theme. Journal of Geophysical Research 110, C1077doi: 101029/2005JC002898.
Roughgarden, J., Gaines, S., Possingham, H., 1988. Recruitment dynamics in complex life cycles. Science 241, 1460–1466.
Shanks, A.L., 1995. Mechanisms of cross-shelf dispersal of larval invertebrates and fish. In: McEdward, L.R. (Ed.), Ecology of Marine Invertebrate Larvae. CRC Press Inc., Boca Raton, Florida, pp. 323–368.
Shanks, A.L., 2009. Pelagic larval duration and dispersal distance revisited. Biological Bulletin 216, 373–385.
Shanks, A.L., Brink, L., 2005. Testing the hypothesis that meroplankton (bivalve larvae) are transported offshore by upwelling. Marine Ecology Progress Series 302, 1–12.
Shanks, A.L., Eckert, G.L., 2005. Population persistence of California Current fishes and benthic crustaceans: a marine drift paradox. Ecological Monographs 75, 505–524.
Shanks, A., Largier, J., Brink, L., Brubaker, J., Hooff, R., 2002. Observations on the distribution of meroplankton during a downwelling event and associated intrusion of the Chesapeake Bay estuarine plume. Journal of Plankton Research 24, 391–416.
Shanks, A.L., Roegner, G.C., 2007. Recruitment-limitation in Dungeness crab populations is driven by temporal variation in climatic forcing. Ecology 88, 1726–1737.
Shanks, A.L., Shearman, R.K., 2009. Paradigm lost? Cross-shelf distributions of intertidal invertebrate larvae are unaffected by upwelling and downwelling. Marine Ecology Progress Series 385, 189–204.
Shenker, J.M., 1988. Oceanographic associations of neustonic larval and juvenile fishes and Dungeness crab megalopae off Oregon. Fishery Bulletin 86, 299–317.
Sinclair, M., 1988. Marine Populations: An Essay on Population Regulation and Speciation. Washington Sea Grant Program, Seattle, Washington, USA.
USGS (U.S. Geological Survey), 2006. National Water Information System. Online interactive database. Available from: ⟨waterdata.usgs.gov⟩ (May 2012).